JACC: CARDIOVASCULAR INTERVENTIONS VOL. 13, NO. 21, 2020

PUBLISHED BY ELSEVIER

Optimal Fluoroscopic Projections of Coronary Ostia and Bifurcations Defined by Computed Tomographic Coronary Angiography

Viktor Kočka, MD, PhD,[a,b,c] Pascal Thériault-Lauzier, MD, PhD,[a] Tian-Yuan Xiong, MBBS, PhD,[a,d] Jeremy Ben-Shoshan, MD, PhD,[a,e] Róbert Petr, MD,[b,c] Marek Laboš, MD,[c] Jean Buithieu, MD,[a] Negareh Mousavi, MD,[a] Thomas Pilgrim, MD,[f] Fabien Praz, MD,[f] Pavel Overtchouk, MD,[a] Jean-Pierre Beaudry, MD,[a] Marco Spaziano, BSc, MD,[a] Jean-Philippe Pelletier, MD,[a] Giuseppe Martucci, MD,[a] Sonny Dandona, MD, PhD,[a] Stéphane Rinfret, MD,[a] Stephan Windecker, MD,[f] Jonathon Leipsic, MD,[g] Nicolo Piazza, MD, PhD[a]

ABSTRACT

OBJECTIVES The aim of this study was to define the optimal fluoroscopic viewing angles of both coronary ostia and important coronary bifurcations by using 3-dimensional multislice computed tomographic data.

BACKGROUND Optimal fluoroscopic projections are crucial for coronary imaging and interventions. Historically, coronary fluoroscopic viewing angles were derived empirically from experienced operators.

METHODS In this analysis, 100 consecutive patients who underwent computed tomographic coronary angiography (CTCA) for suspected coronary artery disease were studied. A CTCA-based method is described to define optimal viewing angles of both coronary ostia and important coronary bifurcations to guide percutaneous coronary interventions.

RESULTS The average optimal viewing angle for ostial left main stenting was left anterior oblique (LAO) 37°, cranial (CRA) 22° (95% confidence interval [CI]: LAO 33° to 40°, CRA 19° to 25°) and for ostial right coronary stenting was LAO 79°, CRA 41° (95% CI: LAO 74° to 84°, CRA 37° to 45°). Estimated mean optimal viewing angles for bifurcation stenting were as follows: left main: LAO 0°, caudal (CAU) 49° (95% CI: right anterior oblique [RAO] 8° to LAO 8°, CAU 43° to 54°); left anterior descending with first diagonal branch: LAO 11°, CRA 71° (95% CI: RAO 6° to LAO 27°, CRA 66° to 77°); left circumflex bifurcation with first marginal branch: LAO 24°, CAU 33° (95% CI: LAO 15° to 33°, CAU 25° to 41°); and posterior descending artery and posterolateral branch: LAO 44°, CRA 34° (95% CI: LAO 35° to 52°, CRA 27° to 41°).

CONCLUSIONS CTCA can suggest optimal fluoroscopic viewing angles of coronary artery ostia and bifurcations. As the frequency of use of diagnostic CTCA increases in the future, it has the potential to provide additional information for planning and guiding percutaneous coronary intervention procedures. (J Am Coll Cardiol Intv 2020;13:2560–70) © 2020 by the American College of Cardiology Foundation.

From the [a]Department of Medicine, Division of Cardiology, McGill University Health Centre, Montreal, Quebec, Canada; [b]Third Faculty of Medicine, Charles University, Prague, Czech Republic; [c]Cardiocenter, University Hospital Královské Vinohrady, Prague, Czech Republic; [d]Department of Cardiology, West China Hospital, Sichuan University, Chengdu, China; [e]Tel-Aviv Medical Center, Sackler School of Medicine, Tel-Aviv University, Tel-Aviv, Israel; [f]Department of Cardiology, Swiss Cardiovascular Center, Bern, Switzerland; and the [g]Department of Radiology, St. Paul Hospital, Vancouver, British Columbia, Canada.

The authors attest they are in compliance with human studies committees and animal welfare regulations of the authors' institutions and Food and Drug Administration guidelines, including patient consent where appropriate. For more information, visit the *JACC: Cardiovascular Interventions* author instructions page.

Manuscript received May 11, 2020; revised manuscript received June 18, 2020, accepted June 19, 2020.

ISSN 1936-8798/$36.00 https://doi.org/10.1016/j.jcin.2020.06.042

Coronary angiography has excellent resolution, but its diagnostic accuracy depends on optimal fluoroscopic projections to avoid foreshortening and overlap of structures. Current recommendations for the most appropriate views are empirical and lack an evidence-based approach (1). Computed tomographic coronary angiography (CTCA) provides a 3-dimensional (3D) representation of the heart and can provide valuable planning information regarding optimal fluoroscopic projections to visualize the ostia of the coronary arteries and proximal bifurcations. Although unknown at this time, CTCA may have a positive impact on clinical outcomes similar to multislice computed tomography-based planning of structural heart disease interventions (e.g., transcatheter aortic valve replacement, transcatheter mitral valve interventions, left atrial appendage occlusion).

CTCA has the potential to influence interventional cardiology practice in several ways: 1) assessment of optimal vascular access; 2) pre-procedural equipment selection (e.g., guiding catheter selection, guidewire type and number, balloon and stent size and length, atherectomy); 3) provision of optimal fluoroscopic viewing angles of aorto-ostial and bifurcation lesions, thereby reducing foreshortening and anatomic overlap (2); 4) selection of percutaneous coronary intervention (PCI) strategy on the basis of lesion characteristics (e.g., culprit artery localization, 1- vs. 2-stent bifurcation stenting, chronic total occlusions); and 5) reduction of the amount of contrast agent volume, radiation exposure, procedural time, complications, and costs (3–5).

Despite increasing frequency of the use of CTCA for diagnostic coronary artery disease, the potential to exploit the same information to guide PCI has been insufficiently investigated. To the best of our knowledge, no study has previously investigated 3D CTCA-based identification of optimal fluoroscopic viewing angles of coronary arteries. The aim of this study was to define optimal fluoroscopic viewing angles of the left coronary artery and right coronary artery (RCA) ostia as well as proximal coronary bifurcations using CTCA.

SEE PAGE 2571

METHODS

STUDY POPULATION. We retrospectively analyzed 100 computed tomographic (CT) coronary angiographic scans of consecutive patients referred for suspected coronary artery disease at University Hospital Královské Vinohrady in Prague. All patients provided written informed consent, and this study was approved by the local ethics committee at University Hospital Královské Vinohrady. All scans were anonymized, and no identifiable patient data were used.

CT CORONARY ANGIOGRAPHIC ACQUISITION. CTCA was performed using a 256-detector-row scanner (Brilliance iCT 256, Philips Medical Systems, Best, the Netherlands). Standard acquisition techniques were applied. In brief, 80 to 100 ml of contrast agent (iodine content 350 to 370 mg/ml) was administered intravenously at a rate of 4 ml/s, oral or intravenous β-blockers were used to control heart rate, and bolus tracking was used for synchronization of contrast medium injection with scanning. Prospective electrocardiographic triggering was the favored modality, scanning 70% to 80% of the RR interval for radiation dose reduction. In patients with high or irregular heart rates (at the discretion of the physician present), retrospective electrocardiographic gating was used. Acquisition was performed with a slice thickness of 0.6 mm.

CT CORONARY ANGIOGRAPHIC ANALYSIS. Using FluoroCT version 3.2 (Circle Cardiovascular Imaging, Calgary, Alberta, Canada) we analyzed the CT coronary angiographic images to define optimal (no foreshortening and overlap of structures) fluoroscopic projections of coronary arteries. Cranial (CRA)/caudal (CAU) and right anterior oblique (RAO)/left anterior oblique (LAO) fluoroscopic views of the C-arm were derived from the sagittal (oblique) and transverse views, respectively.

Analysis of the coronary ostia. After obtaining a centerline of the coronary arteries on multiplanar reconstructions, we identified the perpendicular cross sections of the RCA and left coronary artery ostia. The same operation was repeated to obtain a cross section of the proximal coronary arteries at a distance of 8 mm; this distance was arbitrarily chosen to account for possible foreshortening of the proximal coronary artery segments for this proof-of-concept study. On the perpendicular cross sections of the ostia and 8-mm distance, the coronary artery external limits are marked to generate a round or an ovoid plane. Optimal projection curves provide perpendicular views of a planar structure, similar to what has been reported for the aortic valve annulus during transcatheter aortic valve replacement (6). Optimal projection curves are then computed for the aforementioned coronary planes. The intersection

ABBREVIATIONS AND ACRONYMS

3D = 3-dimensional
CAU = caudal
CI = confidence interval
CRA = cranial
CT = computed tomographic
CTCA = computed tomographic coronary angiography
LAD = left anterior descending coronary artery
LAD-D = left anterior descending coronary artery bifurcation with diagonal branch
LAO = left anterior oblique
LCx = left circumflex coronary artery
LCx-OM = left circumflex coronary artery bifurcation with the obtuse marginal branch
LM = left main coronary artery
LM-LAD-LCx = left main bifurcation into left anterior descending and left circumflex coronary arteries
PCI = percutaneous coronary intervention
PDA-PL = bifurcation into posterior descending artery and posterolateral branch
RAO = right anterior oblique
RCA = right coronary artery

FIGURE 1 Analysis of Optimal Fluoroscopic Viewing Angles for Ostial and Proximal LM Stenting

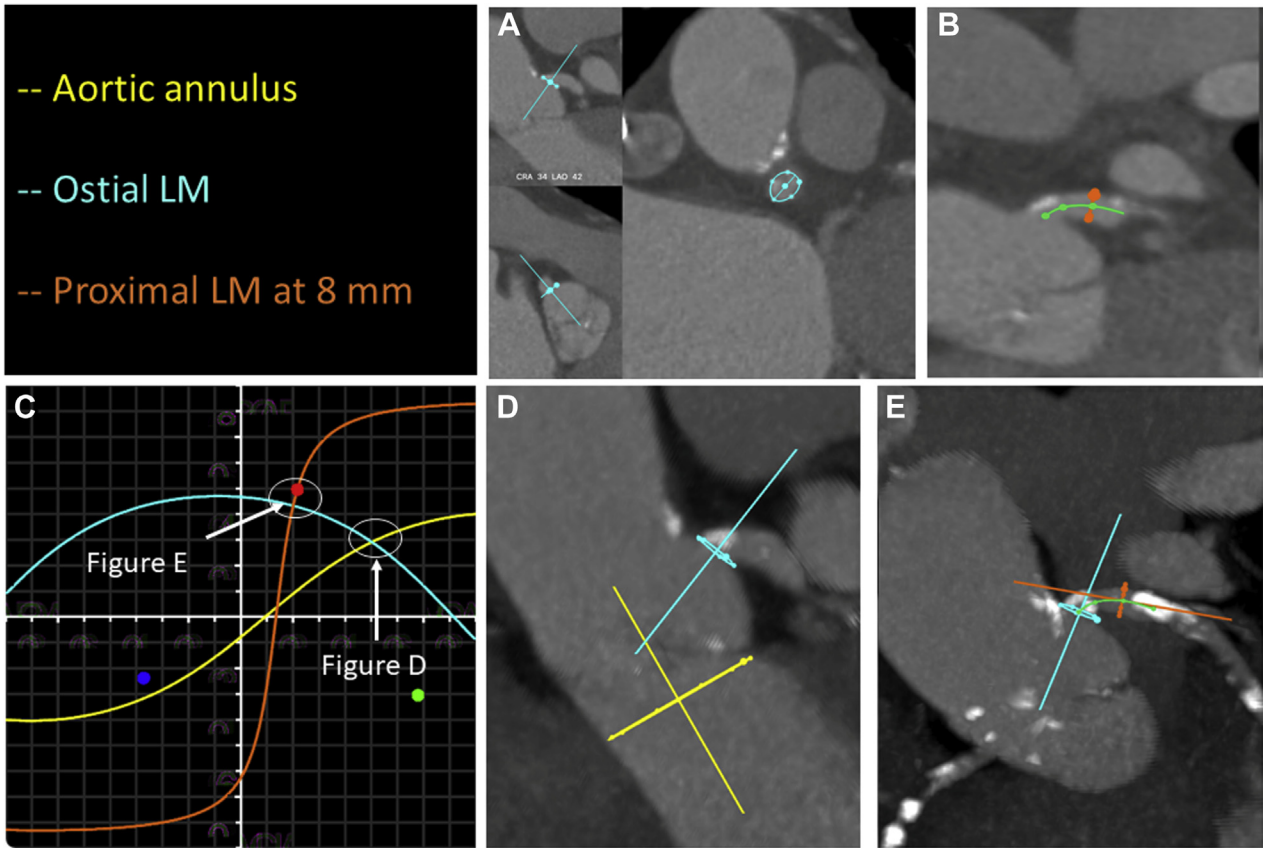

(A) Ostium of the left main coronary artery (LM) is identified in 2 orthogonal planes **(blue closed spline)**. **(B)** A centerline **(green line)** of the LM is created to identify the perpendicular plane of the proximal LM at 8 mm from the ostium. **(C)** Optimal projection curves are then developed for the aortic annulus **(yellow curve)** and the ostial and proximal LM (**blue and orange curves**, respectively). The fluoroscopic viewing angle obtained by the intersection between the aortic annulus and ostial LM optimal projection curves **(D)** mitigates parallax of the aortic root and allows a clear identification of the ostial LM. The fluoroscopic viewing angle obtained by the intersection between the ostial and proximal LM optimal projection curves **(E)** mitigates parallax of the proximal LM. CRA = cranial; LAO = left anterior oblique.

between the optimal projection curves of the ostial left main coronary artery (LM) and aortic annulus (double-S-curve method) provides the optimal fluoroscopic viewing angle for ostial LM stenting. In this view, the aortic annulus and coronary ostia are both in plane while the aortic root is fully elongated, allowing clear visualization of the superior and inferior borders of the coronary ostia with no overlap with contrast in the sinus of Valsalva. The intersection between the optimal projection curves of the ostial LM and proximal LM at 8 mm provides the optimal fluoroscopic viewing angle that would mitigate foreshortening at both stent edges during proximal LM stenting (Figure 1). Similar analyses were conducted for the ostial RCA.

Analysis of the coronary bifurcations. We considered the following coronary bifurcations: 1) LM into left anterior descending coronary artery (LAD) and left circumflex coronary artery (LCx) (LM-LAD-LCx); 2) LAD and first or largest diagonal (LAD-D); 3) LCx and first or largest obtuse marginal branch (LCx-OM); and 4) depending on coronary dominance, RCA or LCx into the posterior descending and posterolateral branches (PDA-PL). Optimal coronary bifurcation angles are computed by creating a 3-point closed spline ("spline" is a mathematical term used to describe a smooth curve passing through defined points) involving the proximal and distal main branch, and side branch, at 5 mm from the polygon of confluence and subsequently calculating

FIGURE 2 Analysis of Optimal Fluoroscopic Viewing Angles of Bifurcating Coronary Arteries

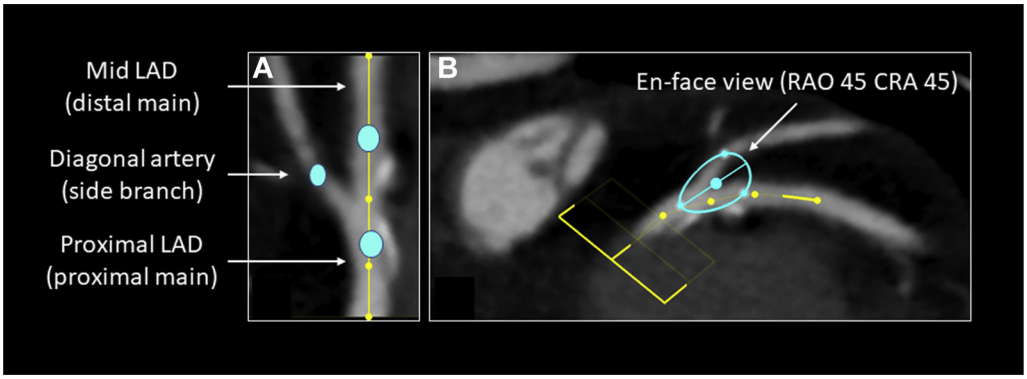

An example of how to obtain the optimal fluoroscopic viewing angle of the bifurcation. A centerline is created in the left anterior descending coronary artery (LAD) at least 5 mm proximally and distally from the diagonal branch take-off. Curved multiplanar reconstruction is used to create a centerline and identify the bifurcation (inlet). The plane or "en face" view of the bifurcation is created by placing 3 dots in the proximal main vessel, distal main vessel, and diagonal branch at 5-mm distance from the polygon of confluence. The "en face" view of the plane provides the optimal fluoroscopic projection for analyzing bifurcation lesions. CRA = cranial; RAO = right anterior oblique.

the en face fluoroscopic viewing angle of that spline. The en face viewing angle of this plane provides optimal assessment of the bifurcation geometry (Figure 2).

Because of physical limitations of current radiographic systems, extreme angulations, although optimal, may not be practical. For the purpose of this study, we have defined a practical projection range within the following limits (highlighted in Figures 3 to 5 by gray stepped lines): for LAO or RAO angle from 0° to 40°, we allowed a maximum CRA or CAU angle of 40°; for LAO or RAO 41° to 60°, we allowed a maximum CRA or CAU angle of 30°; for LAO or RAO 61° to 80°, we allowed a CRA or CAU angle of 20°; and for LAO or RAO 81° to 90°, we allowed a CRA or CAU angle of 10°.

Heart axis calculation. The mitral annulus was identified as previously described by our group (6). In short, the heart axis was measured by a perpendicular line to the plane of the mitral annulus.

STATISTICAL ANALYSIS. Continuous variables are expressed as mean ± SD, and categorical variables are reported as counts and frequencies. Viewing angles are expressed as mean ± 95% confidence interval (CI). Discrepancy between investigators (V.K., T.-Y.X.) was assessed on a randomly selected sample of 10 CT datasets by measuring the angle between viewing planes recorded by each investigator. The Pearson coefficient was used for correlation analysis. Statistical analysis was performed using MATLAB (The MathWorks, Natick, Massachusetts), assuming that the directional data were distributed according to the von Mises-Fisher distribution. A pre-specified sample size of 100 patients was based on experience. The threshold for statistical significance was set at 0.05.

RESULTS

Two of 100 multislice CT scans were not included in the analysis because of poor image quality. Coronary distribution was right dominant in 77 patients (79%), left dominant in 15 patients (15%), and codominant in 6 patients (6%). Table 1 shows mean fluoroscopic projections for all evaluated coronary structures with 95% CIs, interobserver variability analysis, and the percentage of patients within the practical range. No significant associations were found between heart axis and coronary artery structures (all correlation coefficients <0.5).

OSTIAL AND PROXIMAL LM ANALYSIS. LM analysis was complete in 79 patients. Among the 98 patients in whom the analysis was performed, 2 patients had anomalous LCx origin from the right coronary sinus, 1 patient had separate ostia of LAD and LCx, and 16 patients had LM shorter than 8 mm. The optimal projection curves of the aortic annulus and ostial and proximal LM at 8 mm are depicted in Figure 3. The average angle between the planes of the ostial LM and LM at 8 mm was 64°, indicating an element of tortuosity. The average optimal viewing angle for ostial LM stenting was LAO 37°, CRA 22° (95% CI: LAO 33° to 40°, CRA 19° to 25°). The average optimal fluoroscopic

FIGURE 3 Optimal Fluoroscopic Viewing Angles for Ostial and Proximal LM Stenting

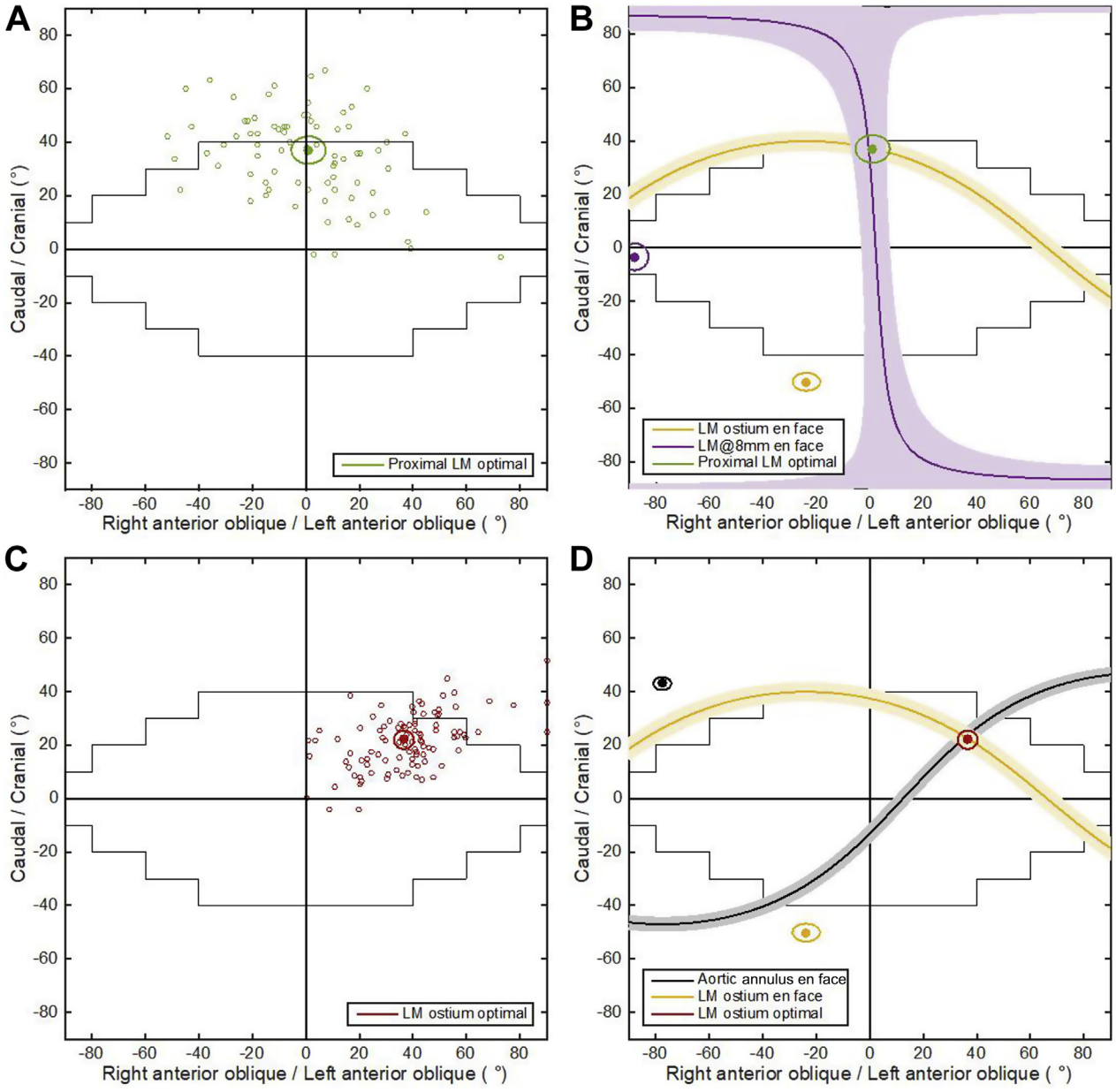

(A) and **(C)** represent scatterplots of individual patients' optimal fluoroscopic viewing angles for stenting the proximal **(green)** and ostial left main coronary artery (LM) **(red)**, respectively. These were obtained using the methods described in Figure 1. The **orange curves in B and D** represent the mean optimal projection curve of the ostial LM with 95% confidence intervals (i.e., views where the ostium of the LM is in plane). The **purple and gray curves in B and D** represent the mean optimal projection curves of the proximal LM at 8 mm and aortic annulus, respectively; the intersection between these curves and the ostial LM projection curve provides the mean optimal fluoroscopic viewing angle for stenting the proximal LM body and ostial LM, respectively. **Gray stepped lines** highlight the practical projection range.

viewing to mitigate foreshortening of the proximal LM up to 8 mm was LAO 1°, CRA 37° (95% CI: RAO 5° to LAO 7°, CRA 32° to 42°). Practical views for ostial and proximal LM stenting would be achievable in approximately 70% of patients (Table 1, Figure 3).

OSTIAL AND PROXIMAL RCA ANALYSIS. Proximal RCA analysis was complete in 97 patients, as 1 patient had an ostial RCA occlusion. The optimal projection curves of the ostial and proximal RCA at 8-mm distance planes are depicted in Figure 4. The

FIGURE 4 Optimal Fluoroscopic Viewing Angles for Ostial and Proximal RCA Stenting

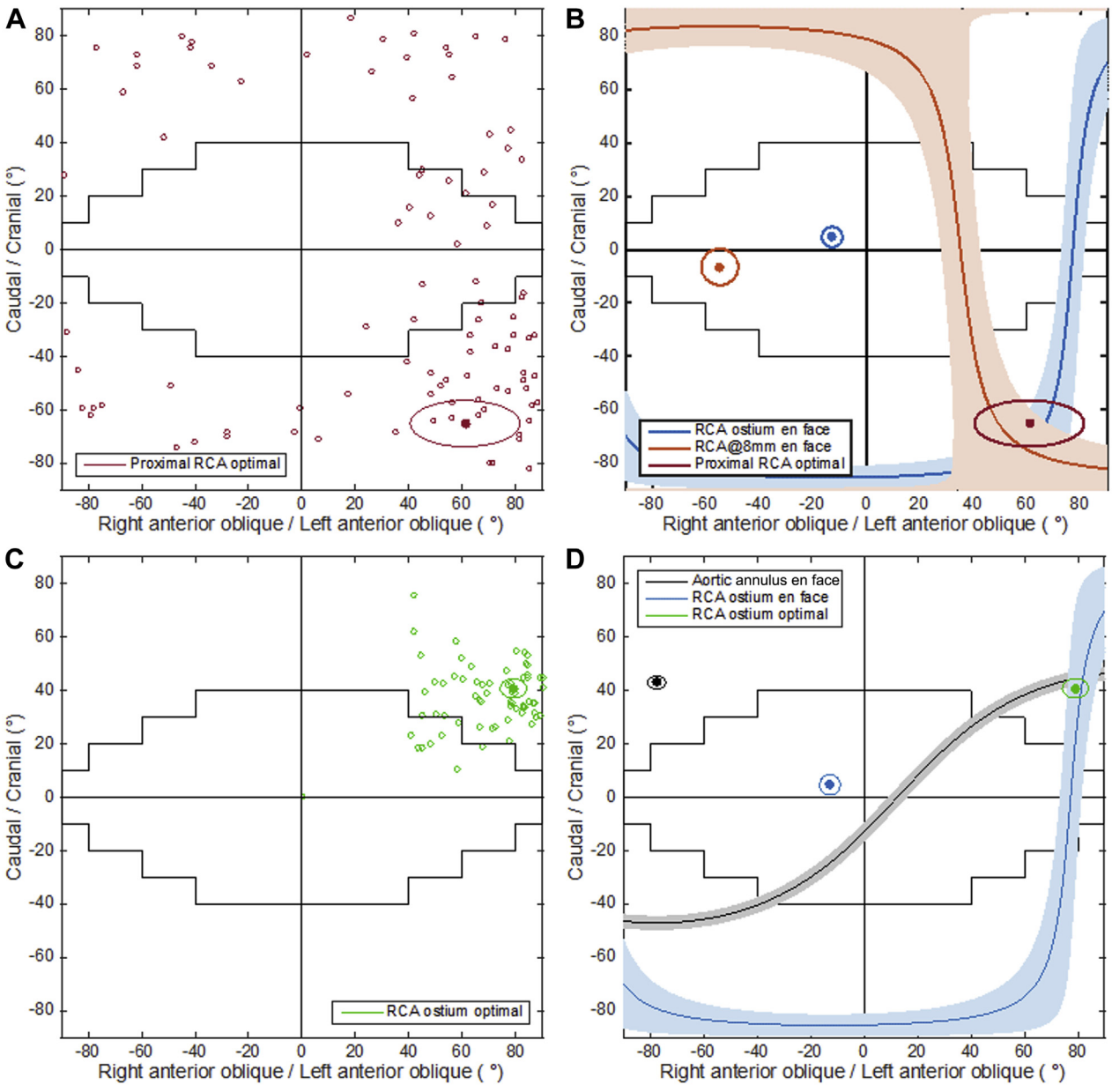

A and C represent scatterplots of individual patients' optimal fluoroscopic viewing angles for stenting the proximal **(red)** and ostial right coronary artery (RCA) **(green)**, respectively. These were obtained using similar methods to those described in Figure 1 for the left main coronary artery. The **blue curves in B and D** represent the mean optimal projection curve of the ostial RCA with 95% confidence intervals (i.e., views where the ostium of the RCA is in plane). The **orange and gray curves in B and D** represent the mean optimal projection curves of the proximal RCA at 8 mm and aortic annulus, respectively; the intersection between these curves and the ostial RCA projection curve provides the mean optimal fluoroscopic viewing angle for stenting the proximal RCA and ostial RCA, respectively. **Gray stepped lines** highlight the practical projection range.

average angle between those 2 planes was 44°, indicating an element of tortuosity. Individual patient data suggest that there is large variability in the perpendicular plane found at 8 mm from the ostium of the RCA (Figure 4A). The average optimal viewing angle for ostial right coronary stenting was LAO 79°, CRA 41° (95% CI: LAO 74° to 84°, CRA 37° to 45°). The average optimal fluoroscopic viewing angle viewing to mitigate foreshortening of the proximal RCA was LAO 64°, CAU 51° (95% CI:

FIGURE 5 Analysis of Coronary Bifurcations

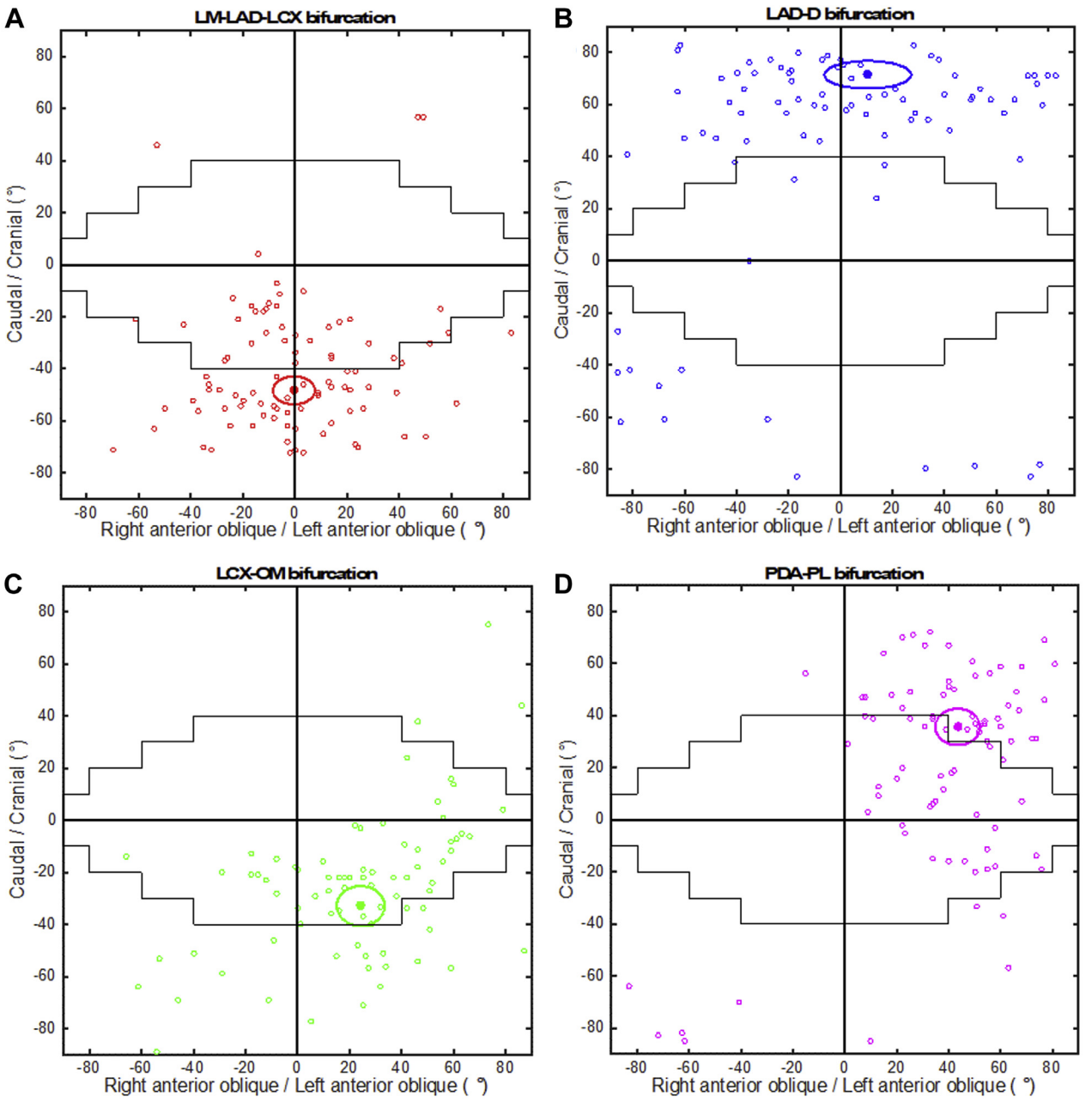

Scatterplots of individual patients optimal fluoroscopic viewing angles for visualizing and stenting bifurcations (the **solid dot** represents the average viewing angle with surrounding 95% confidence interval). **(A)** LM-LAD-LCx bifurcation (left main bifurcation into left anterior descending and left circumflex coronary arteries). **(B)** LAD-D bifurcation (left anterior descending coronary artery bifurcation with diagonal branch). **(C)** LCx-OM bifurcation (left circumflex coronary artery bifurcation with the obtuse marginal branch). **(D)** PDA-PL bifurcation (bifurcation into posterior descending artery and posterolateral branch). **Gray stepped lines** highlight the practical projection range.

LAO 49° to 79°, CAU 42° to 61°). Practical views for ostial proximal RCA stenting would be achievable in approximately 15% of patients (Table 1, Figure 4).

BIFURCATION ANALYSIS. Bifurcation analysis was feasible in: 1) 95 patients for LM-LAD-LCx bifurcation (2 patients were excluded as a result of anomalous origin of the LCx from the right coronary sinus and 1

patient for separate ostia of the LAD and LCx); 2) 85 patients for LAD-D bifurcation (13 patients were excluded as a result of a small or occluded diagonal branch); 3) 80 patients for LCx-OM bifurcation (18 patients were excluded as a result of a small or occluded OM branch); 4) 86 patients for PDA-PL bifurcation (4 patients were excluded as a result of small or occluded branch, 5 patients for codominant coronary distribution, and 3 patients for very high RCA bifurcation).

Estimated mean optimal viewing angles for bifurcation stenting were as follows: LM bifurcation: LAO 0°, CAU 49° (95% CI: RAO 8° to LAO 8°, CAU 43° to 54°); LAD-D: LAO 11°, CRA 71° (95% CI: RAO 6° to LAO 27°, CRA 66° to 77°); LCx bifurcation with first marginal branch: LAO 24°, CAU 33° (95% CI: LAO 15° to 33°, CAU 25° to 41°); and posterior descending artery and posterolateral branch: LAO 44°, CRA 34° (95% CI: LAO 35° to 52°, CRA 27° to 41°). Individual patient plot analysis of all bifurcations suggests that a significant proportion of bifurcation views lie outside the practical projection range (**Figures 5A to 5D, Table 1**). More specifically, only 7% of patients had optimal fluoroscopic projections of the LAD-D bifurcation within the practical range. There was a small difference between the average optimal viewing angle for right- versus left-dominant PDA-PL bifurcations (LAO 44°, CRA 39° [95% CI: LAO 34° to 54°, CRA 31° to 47°] vs. LAO 41°, CRA 18° [95% CI: LAO 21° to 61°, CRA 0° to 37°], respectively).

INTEROBSERVER VARIABILITY. Interobserver variability expressed as mean angle differences between both investigators (V.K., T.-Y.X.) for every measured structure (calculated parameters were not evaluated) is depicted in **Table 1**. Mean angle differences for all bifurcations were very small, all <3°; this reflects the robustness of our methodology. Interobserver variability was also small for measurements of ostial and proximal RCA, but a larger difference was observed in the case of the ostial LM.

TABLE 1 Optimal Fluoroscopic Viewing Angles of Coronary Artery Ostia and Bifurcations

Structure	Fluoroscopic Projection Mean Angle (95% CI)	Interobserver Variability	Within Practical Range
LM			
Optimal projection of LM ostium (n = 95)	LAO 37°, CRA 22° (LAO 33°–40°, CRA 19°–25°)	8.7°	80 (84%)
Optimal projection of proximal LM (n = 79)	LAO 1°, CRA 37° (RAO 5° to LAO 7°, CRA 32°–42°)	9.5°	56 (71%)
RCA			
Optimal projection of RCA ostium (n = 97)	LAO 64°, CAU 51° (LAO 49°–79°, CAU 42°–61°)	1.5°	8 (8%)
Optimal projection of proximal RCA (n = 97)	LAO 79°, CRA 41° (LAO 74°–84°, CRA 37°–45°)	1.1°	16 (16%)
Bifurcations			
LM-LAD-LCx (n = 95)	LAO 0°, CAU 49° (RAO 8° to LAO 8°, CAU 43°–54°)	2.6°	37 (39%)
LAD-D (n = 85)	LAO 11°, CRA 71° (RAO 6° to LAO 27°, CRA 66°–77°)	0.4°	6 (7%)
LCx-OM (n = 80)	LAO 24°, CAU 33° (LAO 15°–33°, CAU 25°–41°)	1.5°	56 (70%)
PDA-PL (n = 86)	LAO 44°, CRA 34° (LAO 35°–52°, CRA 27°–41°)	2.3°	36 (42%)

CAU = caudal; CI = confidence interval; CRA = cranial; LAD = left anterior descending coronary artery; LAD-D = bifurcation of left anterior descending coronary artery and diagonal branch; LAO = left anterior oblique; LCx = left circumflex coronary artery; LCx-OM = bifurcation of left circumflex coronary artery and obtuse marginal branch; LM = left main coronary artery; LM-LAD-LCx = bifurcation of left main coronary artery; PDA-PL = bifurcation of right coronary artery or left circumflex coronary artery into posterior descending artery and posterolateral branch; RAO = right anterior oblique; RCA = right coronary artery.

DISCUSSION

In this study, we describe a CTCA-based method to assess optimal fluoroscopic viewing angles of the coronary ostia and proximal coronary artery bifurcations. The major findings of this study are the following: 1) multiplanar CTCA reconstructions can define optimal fluoroscopic viewing angles for coronary arteries (**Central Illustration**); 2) not all CTCA-defined fluoroscopic viewing angles are practical or achievable with existing C-arm equipment; and 3) across patients, optimal fluoroscopic viewing angles for coronary ostia and bifurcations are highly variable despite a reproducible methodology. In totality, this study suggests that a CTCA-based approach could identify patient-specific optimal fluoroscopic viewing angles of coronary arteries with the purpose to help operators better plan PCI procedures.

During the 1970s and early 1980s, anecdotal experience defined the current fluoroscopic viewing angles to appreciate various aspects of the coronary arterial tree (7–10). With the introduction of mobile C-arms, the well-known nomenclature "RAO/LAO and CRA/CAU" became standard vernacular in the early 1980s (9,11). Computer modeling with complex mathematics was used to provide a 3D reconstruction of coronary arteries from several angiographic projections or rotational angiography (12) (U.S. patent 6501848 B1). This technique was then used to provide the first scientifically based optimal views of coronary segments, but ostial and bifurcation lesions were difficult to study (13). Although recent studies have demonstrated the ability to "fuse" invasive coronary angiography with various invasive and noninvasive imaging modalities (e.g., computed tomography, optical coherence tomography), none of these have evaluated a patient-specific approach using CTCA to generate optimal fluoroscopic viewing angles of coronary arteries (14–17).

CENTRAL ILLUSTRATION **Optimal Fluoroscopic Viewing Angles of Coronary Artery Ostia and Bifurcations**

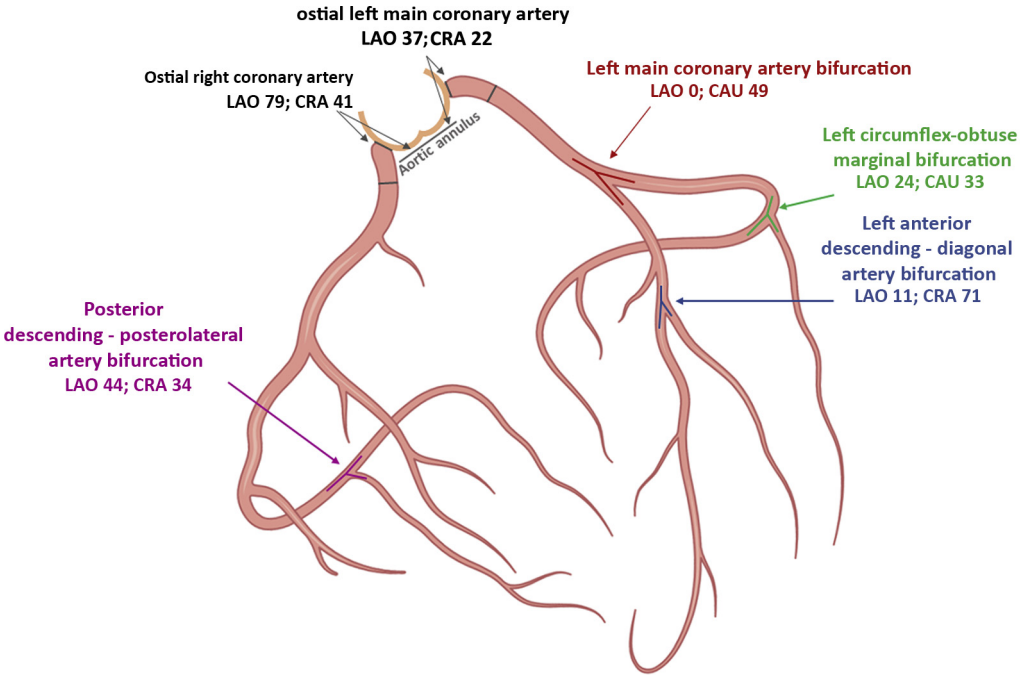

Kočka, V. et al. J Am Coll Cardiol Intv. 2020;13(21):2560–70.

CAU = caudal; CRA = cranial; LAO = Left anterior oblique.

Standard angiographic projections are not uncommonly associated with vessel foreshortening and vessel overlap. Longitudinal geographic miss may follow inappropriate stent length selection or placement and is of particular importance in ostial lesions (i.e., aortic or side branches), in which the incidence of inaccurate stent placement can vary from 54% to 87% (3,4,18). Patients with longitudinal geographic miss have 2 to 3 times the rate of target vessel revascularization as patients without this issue (4,5). Stent length excess is also associated with worse outcomes, increasing the likelihood of late luminal loss and longitudinal stent deformation (19,20). The double-S-curve method to define optimal viewing angles of the left and right coronary ostia naturally provides isolation and elongation of the left and right coronary cusps, thereby mitigating the effects of sinus overlap or foreshortening. In fact, the double-S-curve method provides the aortic annulus in plane, and for this reason the aortic root (or sinus of Valsalva) is not foreshortened. The right and noncoronary cusps are overlapped in the optimal view of the left coronary artery ostium, while the left and noncoronary cusps are overlapped in the optimal view of the RCA ostium. Future studies should investigate whether CTCA-based PCI planning can mitigate complications such as geographic miss or inappropriate stent length selection. From a more general perspective, the CTCA-derived fluoroscopic images could after coregistration be visible to the operator, and the optimal shape and size of a guiding catheter could be selected on the basis of individual patient anatomy.

By appreciating the scatterplots and optimal projection curves, the present study provides operators with a potential strategic plan to guide PCI even in the absence of pre-procedural CTCA. For example, operators could perform 3 coronary test injections during LM bifurcation stenting: 1) RAO 20°, CAU 40°; 2) LAO 0; CAU 40°; and 3) LAO 20°, CAU 40°. For ostial LM stent positioning, operators should remain within the boundaries of LAO 30° to 40° and CRA 20° to 25°. For ostial right coronary stent positioning, operators should strive for LAO 75° to 85°, with as much CAU angulation as possible (CRA 35° to 45°). This systematic approach to coronary test injections based on a series of CT coronary angiographic analyses may provide the operator with a more efficient means to approaching everyday PCI.

Figures 5A to 5D are scatterplots of patients depicting optimal fluoroscopic viewing angles for bifurcation stenting. Our data suggest that an

optimal fluoroscopic viewing angle of the LAD-D bifurcation is achievable in a small minority of patients (<10%) (Table 1). This suggests that in the vast majority of patients, the limbs of the LAD-D bifurcation are foreshortened, and their ostia may be difficult to visualize. Consequences of poor visualization may include the risk for incomplete side branch stent overage or protrusion of the side branch stent into the main vessel, causing obstruction of the main branch. Therefore, during LAD-D bifurcation stenting, the operator may select a stenting technique that considers the potential foreshortening and provides proper stent coverage of the ostial side branch (e.g., double-kissing crush). In contrast, an operator may have a better chance (71%) of obtaining an optimal fluoroscopic viewing angle during LCx-OM bifurcation stenting with greater confidence in positioning a stent at the true ostium of the side branch, thereby selecting a bifurcation stenting technique that reduces metal overlap (e.g., T and protrusion stenting).

STUDY LIMITATIONS. This was a retrospective study that evaluated the feasibility of CTCA to provide optimal fluoroscopic viewing angles of the coronary arterial tree and did not evaluate the clinical impact of this approach (e.g., contrast volume, radiation exposure, procedural duration, cardiovascular event rates). Although optimal fluoroscopic viewing angles may not be practical for all (e.g., LAD-D bifurcation), this might also suggest that some amount of foreshortening during PCI is inevitable. Although previous data suggest that the presence of coronary guidewires during PCI may modify the bifurcation angle to some degree (21), we suspect that this will have little if any impact on optimal fluoroscopic viewing angles predicted by CTCA. Extreme angulations are not only difficult to achieve but also result in an increased radiation dose and decreased image quality. Although yet to be confirmed, coronary motion and a patient's position on the catheterization laboratory table may have an impact on the precision of CTCA to define optimal fluoroscopic viewing angles of coronary arteries. Anecdotal experience and published work using computed tomography to define optimal fluoroscopic viewing angles for structural heart interventions would suggest that cardiac motion and a patient's position on the catheterization laboratory table relative to the CT table would have little impact on the precision of CTCA to define optimal fluoroscopic viewing angles of coronary arteries.

CONCLUSIONS

Herein, we report a 3D CTCA-based method to analyze optimal fluoroscopic viewing angles of the coronary arteries intended to assist operators for coronary angiography and staged PCI procedures. Given the increasing use of CTCA for diagnostic and prognostic purposes, the proposed approach could be integrated in the usual work flow and provide patient-specific, individualized information to PCI operators. Future efforts should focus on studies assessing the agreement between predicted tomographic optimal viewing angles and invasive angiography and the impact it may have on clinical outcomes.

AUTHOR RELATIONSHIP WITH INDUSTRY

Dr. Kočka was supported by the European Commission: 1) Operational Programme: Research, Development and Education, Summons No. 17 International Mobility of Researchers (CZ.02.2.69/0.0/0.0/16_027/0008495); 2) Operational Programme: Research, Development and Education, project INTERCARDIS (CZ.02.1.01/0.0/0.0/16_026/0008388); and by Charles University Research Centre (UNCE/MED/002). Drs. Thériault-Lauzier and Piazza have been consultants for Circle Cardiovascular Imaging. All other authors have reported that they have no relationships relevant to the contents of this paper to disclose.

ADDRESS FOR CORRESPONDENCE: Dr. Nicolo Piazza, Division of Cardiology, Department of Medicine, McGill University Health Centre, The Royal Victoria Hospital, 1001 Boulevard Décarie, Montréal, QC H4A 3J1, Canada. E-mail: nicolopiazza@mac.com.

PERSPECTIVES

WHAT IS KNOWN? Routine fluoroscopic projections used for coronary angiography have an empirical basis and require refinements by iterative contrast injections.

WHAT IS NEW? In this study, we provide CTCA-based optimal fluoroscopic viewing angles of the coronary ostia and proximal coronary artery bifurcations using novel methods including optimal projection curves of coronary arteries.

WHAT IS NEXT? Future efforts should focus on studies assessing the agreement between predicted tomographic optimal viewing angles and invasive angiography and the impact it may have on clinical outcomes.

REFERENCES

1. Di Mario C, Sutaria N. Coronary angiography in the angioplasty era: projections with a meaning. Heart 2005;91:968–76.

2. Burzotta F, De Vita M, Sgueglia G, Todaro D, Trani C. How to solve difficult side branch access? EuroIntervention 2010;6 suppl J:J72–80.

3. Rubinshtein R, Ben-Dov N, Halon DA, et al. Geographic miss with aorto-ostial coronary stent implantation: insights from high-resolution coronary computed tomography angiography. EuroIntervention 2015;11:301–7.

4. Dishmon DA, Elhaddi A, Packard K, Gupta V, Fischell TA. High incidence of inaccurate stent placement in the treatment of coronary aorto-ostial disease. J Invasive Cardiol 2011;23:322–6.

5. Costa MA, Angiolillo DJ, Tannenbaum M, et al. Impact of stent deployment procedural factors on long-term effectiveness and safety of sirolimus-eluting stents (final results of the multicenter prospective STLLR trial). Am J Cardiol 2008;101:1704–11.

6. Spaziano M, Theriault-Lauzier P, Meti N, et al. Optimal fluoroscopic viewing angles of left-sided heart structures in patients with aortic stenosis and mitral regurgitation based on multislice computed tomography. J Cardiovasc Comput Tomogr 2016;10:162–72.

7. Arani DT, Bunnell IL, Greene DG. Lordotic right posterior oblique projection of the left coronary artery: a special view for special anatomy. Circulation 1975;52:504–8.

8. Miller RA, Warkentin DL, Felix WG, Hashemian M, Leighton RF. Angulated views in coronary angiography. AJR Am J Roentgenol 1980;134:407–12.

9. Sos TA, Baltaxe HA. Cranial and caudal angulation for coronary angiography revisited. Circulation 1977;56:119–23.

10. Aldridge HE. Better visualization of the asymmetric lesion in coronary arteriography utilizing cranial and caudal angulated projections. Chest 1977;71:502–7.

11. Grover M, Slutsky R, Higgins C, Atwood JE. Terminology and anatomy of angulated coronary arteriography. Clin Cardiol 1984;7:37–43.

12. Chen SJ, Carroll JD. 3-D reconstruction of coronary arterial tree to optimize angiographic visualization. IEEE Trans Med Imaging 2000;19:318–36.

13. Garcia JA, Movassaghi B, Casserly IP, et al. Determination of optimal viewing regions for X-ray coronary angiography based on a quantitative analysis of 3D reconstructed models. Int J Cardiovasc Imaging 2009;25:455–62.

14. Gollapudi RR, Valencia R, Lee SS, Wong GB, Teirstein PS, Price MJ. Utility of three-dimensional reconstruction of coronary angiography to guide percutaneous coronary intervention. Catheter Cardiovasc Interv 2007;69:479–82.

15. Green NE, Chen SY, Hansgen AR, Messenger JC, Groves BM, Carroll JD. Angiographic views used for percutaneous coronary interventions: a three-dimensional analysis of physician-determined vs. computer-generated views. Catheter Cardiovasc Interv 2005;64:451–9.

16. Messenger JC, Chen SY, Carroll JD, Burchenal JE, Kioussopoulos K, Groves BM. 3D coronary reconstruction from routine single-plane coronary angiograms: clinical validation and quantitative analysis of the right coronary artery in 100 patients. Int J Card Imaging 2000;16:413–27.

17. Hecht HS. Applications of multislice coronary computed tomographic angiography to percutaneous coronary intervention: how did we ever do without it? Catheter Cardiovasc Interv 2008;71:490–503.

18. Jaffe R, Halon DA, Shiran A, Rubinshtein R. Percutaneous treatment of aorto-ostial coronary lesions: current challenges and future directions. Int J Cardiol 2015;186:61–6.

19. Mauri L, O'Malley AJ, Cutlip DE, et al. Effects of stent length and lesion length on coronary restenosis. Am J Cardiol 2004;93:1340–1346, A5.

20. Williams PD, Mamas MA, Morgan KP, et al. Longitudinal stent deformation: a retrospective analysis of frequency and mechanisms. EuroIntervention 2012;8:267–74.

21. Sawaya FJ, Lefevre T, Chevalier B, et al. Contemporary approach to coronary bifurcation lesion treatment. J Am Coll Cardiol Intv 2016;9:1861–78.

KEY WORDS computed tomography, coronary angiography, coronary arteries, fluoroscopy, percutaneous coronary intervention